Hindawi
Geofluids
Volume 2020, Article ID 8859309, 12 pages
https://doi.org/10.1155/2020/8859309

Research Article

Study on the Origin and Fluid Identification of Low-Resistance Gas Reservoirs

Zhou Yuhui,[1,2] **Hu Qingxiong**,[3] **Liu Wentao**,[4] **Wu Zhiqi**,[5] **Yan Yule**,[2] **and Ma Jialing**[1]

[1]*Yangtze University, Wuhan, Hubei, China 430100*
[2]*National Coal Chemical Product Quality Supervision and Inspection Center, Huainan, Anhui, China 232001*
[3]*The No.1 Oil Production Plant, PetroChina Xinjiang Oilfield Company, Karamay, Xinjiang, China 834000*
[4]*Research Institute of Exploration and Development, Xinjiang Oilfield Company, PetroChina, Karamay, Xinjiang, China 834000*
[5]*Heavy Oil Company, PetroChina Xinjiang Oilfield Company, Karamay, Xinjiang, China 834000*

Correspondence should be addressed to Zhou Yuhui; zhyhtree@yangtzeu.edu.cn

Received 18 August 2020; Revised 1 November 2020; Accepted 17 November 2020; Published 2 December 2020

Academic Editor: Shiyuan Zhan

The Wu 2 section of the Ke017 well block is a low-resistance gas reservoir with ultralow porosity and low permeability. The comprehensive analysis of rock lithology, physical properties, sedimentary characteristics, and gas content demonstrated that the development of micropores in illite/smectite dominated clay minerals together with the resulted additional conductivity capability and complex reservoir pore structures, as well as the enrichment of self-generating conductivity minerals like zeolites and pyrite which were the formation mechanisms of low-resistance gas layers in the Wu 2 section. A low-resistance gas reservoir has poor physical property, and it is difficult to distinguish the oil layer from the dry, gas, or water layers. In this paper, based on well/mud logging data and laboratory data, by taking advantages of the "excavation effect" of neutron gas and the dual-lateral resistivity difference between different depths, we successfully established a set of low-contrast log response methods for the identification and evaluation of oil layer and formation fluids. For a gas layer, the difference between neutron porosity and acoustic (or density) porosity is smaller than 0 and the difference in dual-lateral resistivity is greater than 0. For a water layer, the neutron porosity is similar to the acoustic (or density) porosity and the dual-lateral resistivity difference will be less than 0. While for a dry layer or a layer with both gas and water, the difference in porosity as well as dual-lateral resistivity is very small. The proposed method effectively solves the technical problem of oil layer and formation fluid identification in low-resistance gas reservoirs.

1. Introduction

A low-resistance oil/gas reservoir is defined as the oil/gas reservoir with a resistivity ratio between oil/gas layer and water layer smaller than 2 [1]. It is an important and promising exploration field of subtle oil and gas reservoirs, which are mostly deposited in reservoirs with fine grain sizes and high shale content that formed under the weak hydrodynamic interactions of delta, shore-shallow lacustrine, and turbidite fan and located in low-amplitude tectonic regions [2–5]. Due to the effects of high immobile water saturation, additional conductivity of clay minerals, conductive minerals, oil-water differentiation, oil-water layer salinity difference, and drilling fluid intrusion, the resistivity of oil and gas layer in low-resistance oil/gas reservoir is generally lower than that of conventional oil and gas layer [6, 7]. As a result, during logging interpretation, it is easy to confound the oil/gas layer with water layer and miss the potential production layer. Therefore, it is urgent to find a suitable and reliable interpretation method for low-resistance oil and gas layer and promote the development of such kind of oil and gas reservoirs [8]. Researchers have done a lot of research work to resolve this problem. The main methods they applied may include the mobile water method [9], multivariate statistical method [10, 11], W-S saturation based model method [12], dual-porosity superposition [13], elastic parameters method [14], dual water model method [15], and array acoustic/induction/nuclear magnetic resonance logging evaluation method

[16–21]. Most researchers tended to pay more attention to special logging technologies so as to find out a quantitative method for fluid identification in low-resistance reservoirs, and there was scarce information on using conventional logging data. Due to the effects of poor reservoir conditions and low oil recovery, the researches on the formation mechanism and log identification and evaluation of the low-resistance gas reservoir in upper Wuerhe formation of Permian in Zhungeer basin are still insufficient. The Wu 2 member of Ke017 block in this area is a typical low-resistance glutinite gas reservoir with complex pore structure, ultralow porosity and permeability, and low salinity. There is no special logging data; only conventional logging data are available. In this paper, we established a set of low-contrast log response methods for the identification and evaluation of oil layer and formation fluids by analyzing the formation mechanisms and governing factors.

2. Geological Characteristics of Gas Reservoirs

The Ke017 well area is located in the lower plate of the Karamay Dainian fault in the western uplift of the Junggar Basin, East of Zhongguai. Before the deposition of the Upper Urhe Formation of the Permian in the Zhonggua uplift, uneven development occurred before deposition, the paleo-convex divided the water system, and the three fan delta depositional systems developed. From south to north, they are the Zhongguai fan, Karamay fan, and Baijian beach fan. Well Ke017 is located at the northwestern edge of the Zhongguai fan. The parent rock is dominated by volcanic debris, which is near the provenance of large-scale shallow-water degenerate fan delta and has strong hydrodynamic force. The reservoir lithology is complex, including conglomerate, glutenite, and sandstone. The reservoir has poor physical properties, with a porosity of 3.20% to 14.63%, an average of 6.50%, a permeability of 0.43 to 211.12 mD, and an average of 6.31 mD. Moreover, it belongs to low-resistance gas reservoirs with complex lithology, extralow porosity, and low permeability. Its gas layer has poor physical properties (wells need fracturing to obtain productivity), low resistivity, and a resistivity increase rate; therefore, it is easy to confuse with the dry and water layers and is extremely difficult to identify.

3. Genesis Mechanism of Low Gas Barrier

3.1. Higher Content of Illite/Montmorillonite Mixed Layer. According to the core microscopic scanning electron microscopy (Figure 1), the clay minerals in the Wu 2 member of the reservoir in this area mainly have irregular grain-like, honeycomb-like illite/montmorillonite mixed minerals and a small amount of wire-like, bridging illite. The irregular, honeycomb-like illite/montmorillonite mixed layers have micropores, through which they can absorb a large amount of formation water to form bound water. The wire-shaped, bridge-shaped illite can also absorb a lot of formation water to form bound water; therefore, the gas trapped-water content is high.

According to X-ray diffraction analysis (Table 1), statistics show that the content of the illite/montmorillonite mixed layer+illite in this area is 2.8 to 10.0%, with an average of 6.0%, with relatively high content. The structural charge of montmorillonite comes from the substitution of Al^{3+} by Mg^{2+} and Fe^{2+} ions in the octahedron sheet. The structural charge of illite comes from the replacement of Si^{4+} in the silicon tetrahedron sheet by Al^{3+}, resulting in a higher negative charge for this type of mineral. Under the action of an external electric field, a large amount of cations in the formation water will be adsorbed on the surface of the illite/montmorillonite mixed layer, which will cause greater additional conductivity and reduce the resistivity rapidly.

The high content of the illite/montmorillonite mixed layer is one of the most important reasons for the formation of the low gas barrier layer in the Wu 2 member of this area.

3.2. Complex Pore Structure. The parent rock of the second member of the Upper Urhe Formation of the Permian in this area is dominated by volcanic debris and is a near-source, large-scale shallow-water degenerate fan delta front deposit. The reservoir is mainly composed of tuff lithic sandstone and glutenite with an unequally grained sandy structure. Its classification is medium to poor, its roundness is subcircle to angular, and the maturity of the components and structure is low. According to the statistics of the analysis results of the cast body sheet (Figure 2), the pore types are mainly secondary pores, including intergranular dissolved pores, interface pores, and microcracks, a small amount of muddy dissolved pores, and the average pore diameter is 10.44~66.44 μm, with an average of 40.92 μm (Table 2); the pore diameter is small, and it is dominated by fine pores.

Mercury pressure data show that the capillary pressure curve of the reservoir of the Wu 2 section in this area is mainly a fine distortion; its driving pressure is large, and the pore sorting is poor. The maximum pore throat radius is 0.01~5.9 μm with an average of 2.68 μm; expulsion pressure is 0.12 to 0.85 MPa with an average of 0.46 MPa; saturated median pressure is 0.27 to 18.12 MPa with an average of 6.89 MPa; saturated median radius is 0.13 to 2.76 μm with an average of 0.59 μm; unsaturated pore volume is 18.00% to 66.27%, with an average of 48.25%; and mercury removal efficiency is 13.14% to 43.64%, with an average of 22.93% (Figure 3).

Comprehensive analysis shows that the Wu 2 section in this area is a fan delta sediment, which has large reservoir particle changes and a complex primary pore structure. Under the diagenesis of compaction, cementation, and dissolution, and after more complicated diagenetic changes, the primary pores are compacted significantly and the residual pores are few. The secondary pores are mainly developed, the pores are microporous and complicated, the pore throat diameter is small, and fine pores are abundant. The displacement pressure is high and the rocks' ability to retain formation water is strong. Formation water in the capillaries is insufficiently displaced and left in the tiny pore throat, resulting in high saturation of the bound water.

The complex reservoir pore structure is one of the important reasons for the formation of the low gas barrier in the Wu 2 section of this area.

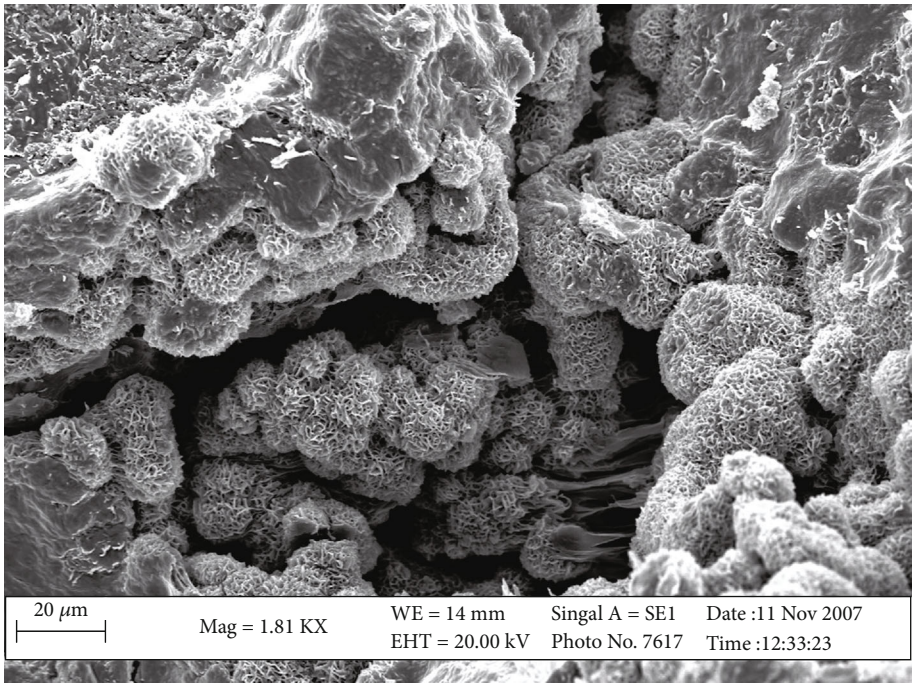

(a)

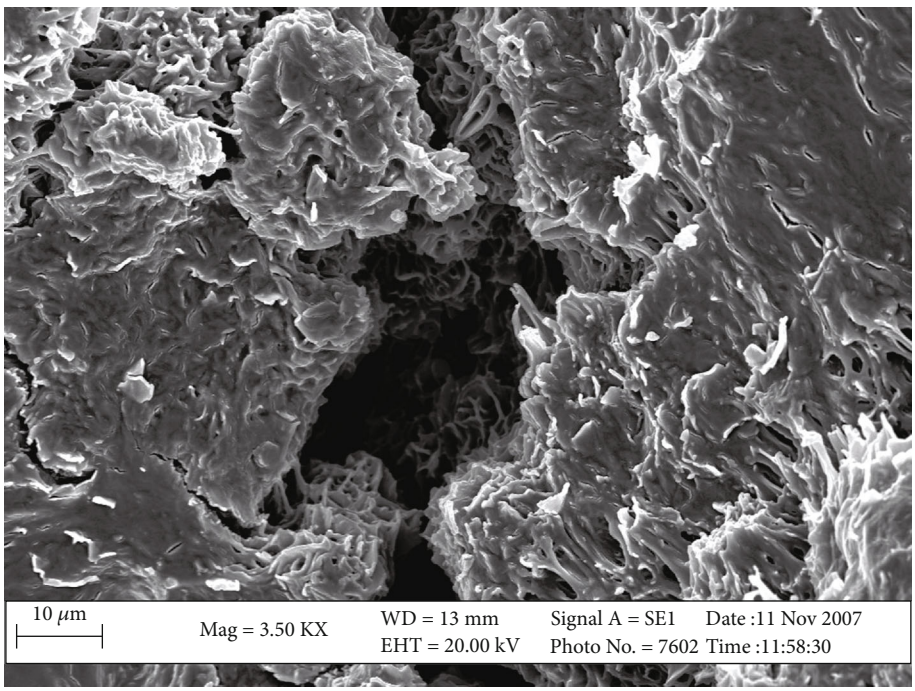

(b)

Figure 1: Continued.

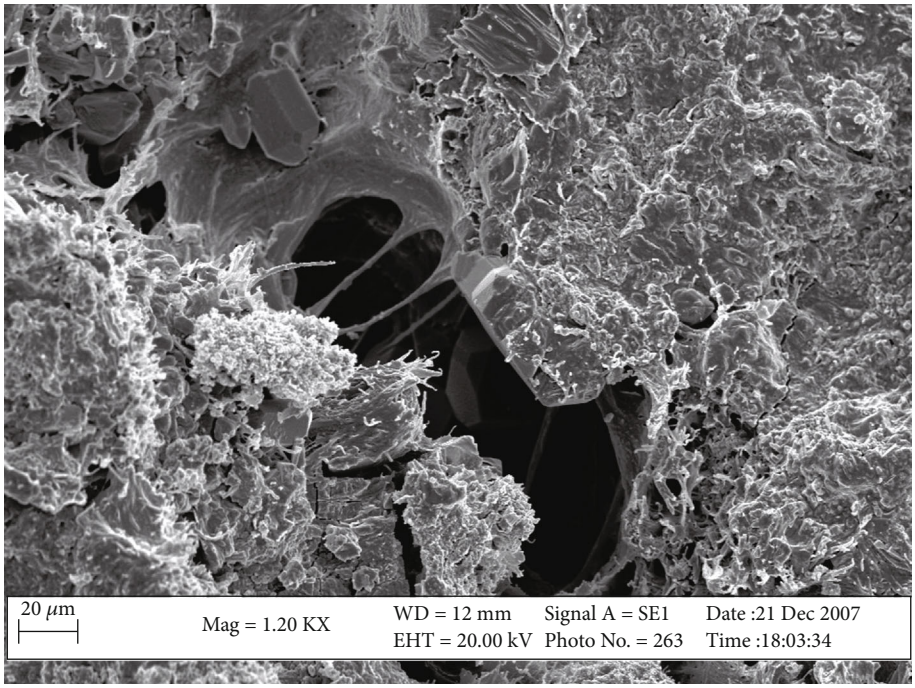

(c)

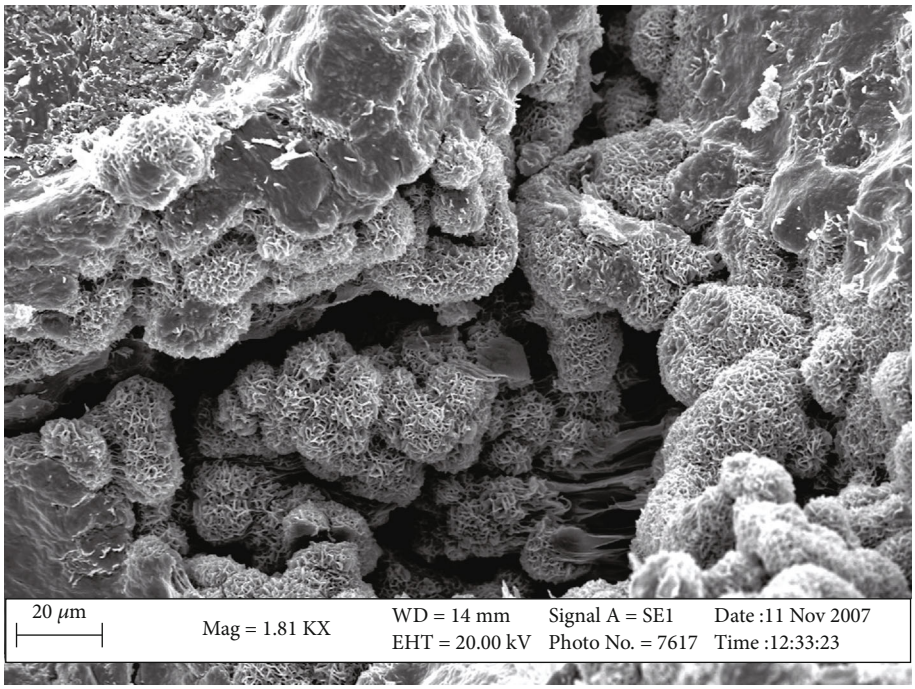

(d)

Figure 1: Scanning electron microscope picture of the second Wu member of well 017. (a) W1, 3094.33 m, the intergranular filling in illite/montmorillonite mixed-layer minerals; (b) W3, 3361.37 m, dissolved pore-filled I illite/montmorillonite mixed-layer minerals; (c) W1, 3099.27 m, intergranular filling of illite/montmorillonite mixed-layer minerals and bridging illite; (d) W3, 3364.67 m, intergranular pores and grain-like honeycomb illite/montmorillonite mixed-layer minerals.

3.3. Rich in Zeolites and Pyrite Authigenic Minerals. According to the core microscanning electron microscope (Figure 4), there are more zeolites and pyrite authigenic minerals in the pores. Zeolite is a kind of hydrous alkali metal or alkaline earth metal-containing aluminosilicate mineral, which has the characteristics of ion exchange, conductivity, adsorption and separation, reversible dehydration, etc., that can reduce the formation resistivity. Pyrite is a metal with good conductivity, which can reduce the reservoir resistivity.

The abundance of zeolites and pyrite authigenic conductive minerals is also one of the reasons for the formation

Table 1: X-ray diffraction quantitative analysis statistics table of Wu 2 section in well Ke017.

Well	The sample depth (m)	Horizon	Lithology	Clay content (%)	Clay mineral content (%)				I/S+I content (%)
					I/S	I	K	C	
Jin long 26	3005.93	P_3W_2	Glutenite	3.26	83	3	2	12	2.80
Ke011	3247.6	P_3W_2	Glutenite	11.92	82	2	3	13	10.0
Ke011	3251.2	P_3W_2	Glutenite	5.87	85	2	2	11	5.11
Ke011	3261.7	P_3W_2	Glutenite	6.82	80	3	2	15	5.66
Average				6.97	83	3	2	13	5.99

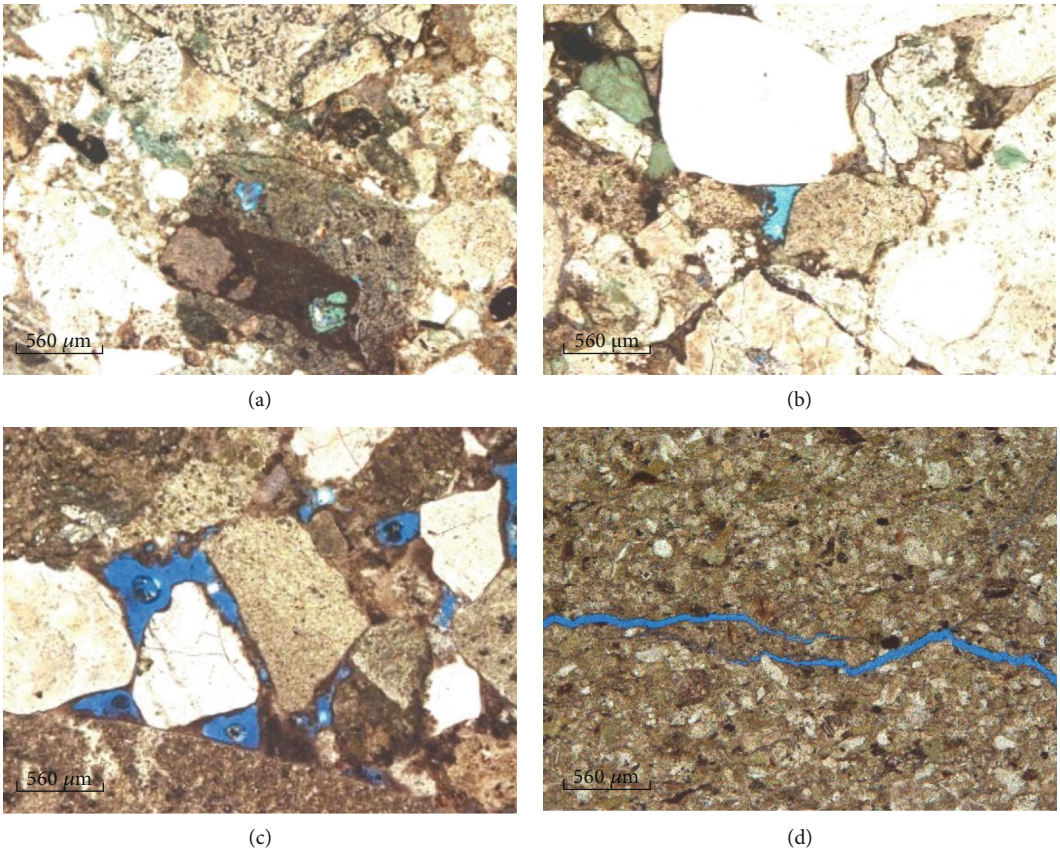

Figure 2: Photograph of a thin slice of the Wu 2 section in the Ke017 well area. (a) Jin long 26, 3006.9 m, intragranular pores; (b) Jin long 26, 3009.75 m, residual intergranular pore; (c) Mahu 8, 3353.2 m, residual intergranular pore; (d) Jin long 26, 3005.41 m, microcrack.

of the low-resistivity gas reservoirs of the Wu 2 section in this area.

4. The Main Control Factors of Forming Low-Resistivity Gas Reservoir

The low-resistance gas layer is formed by the comprehensive response of many factors such as structure, sedimentation, lithology, physical properties, gas-bearing properties, and formation water.

The Wu 2 section in this area is near the provenance of large-scale shallow-water degenerate fan delta sediments. The parent rock is mainly composed of volcanic debris, and the reservoir lithology is complex. It mainly contains conglomerate, sandy small conglomerate, glutenite, pebbly argillaceous fine sandstone, pebbly unequal grain sandstone, pebbly argillaceous sandstone, and siltstone. Grain sorting is medium to poor, and the particle degree of roundness is mainly from subround to edges. Composition maturity and structure maturity are low. The structure of the primary pore is complex. Under the action of overlying pressure, it is easy to be compacted and the less primary pore remains.

The depth of the central Wu 2 gas reservoir in this area is 3200 m, the formation pressure of the gas reservoir is 40 MPa, and the formation temperature is 81.5°C; it has experienced complex diagenesis. The reservoir structure is relatively compact, compaction is strong, the particles are in point-line contact, and the cementation type is the pore pressure inlay type.

Table 2: Analysis and statistics table of thin section castings in the Wu 2 section in Ke017 well area.

Well	Depth (m)	Lithology	Structure	Pore types	Face rate (%)	Homogeneous coefficient	Sorting coefficient	Average pore diameter (μm)
Jin long 26	3005.41	Glutenite	Very fine sand texture	Microcrack	/	/	/	/
Jin long 26	3006.9	Sandstone	Gravel bearing unequal sandy structure	Intragranular pores	0.06	0.63	27.37	48.67
Jin long 26	3008.35	Argillaceous fine sandstone	Unequal sandy structure	Intragranular pores	0.05	0.29	8.46	10.44
Jin long 26	3009.75	Glutenite	Gravel bearing unequal sandy structure	Residual intergranular pore	0.14	0.61	39.96	66.44
Jin long 26	3010.84	Glutenite	Gravel bearing unequal sandy structure	Residual intergranular pore Intragranular pores Microcrack	0.29	0.32	32.90	34.86
Jin long 26	3012.14	Grit	Gravel unequal sandy structure	Residual intergranular pore Intragranular pores	0.15	0.44	32.76	44.17
Average					0.14	0.46	28.29	40.92

The pore types are mainly secondary pores, including intergranular solution pores, interface pores and microfractures, and a small amount of muddy medium solution pores; its diagenetic stage is in the late diagenetic stage A. Under the action of compaction, cementation, dissolution, and other diagenesis, the degree of diagenetic heterogeneity is strong, which makes the pore structure of the reservoir more complex and a large number of pores are microporous. The clay mineral montmorillonite was converted to the Iranian/Mongolian mixed layer in large quantities; zeolites and pyrite authigenic minerals were formed in the original pores. Finally, a variety of genesis was superimposed to form the low-barrier gas layer of the Wu 2 section in this area.

Therefore, the fan delta depositional system and complex diagenesis near the provenance are the main controlling factors for the formation of low-resistivity gas reservoirs of the Wu 2 section in this area.

5. Effective Reservoir and Fluid Identification

According to the gas-bearing property of the reservoir, the low-resistivity gas reservoir in the second member of Wuhe formation can be divided into gas, gas-water, water, and dry layers. However, the reservoir condition is poor (the porosity of the effective reservoir is similar to that of the dry reservoir). The low increase rate of resistance, that is, the resistivity of gas and water layers, is similar. Conventional methods such as resistivity and porosity cannot effectively distinguish effective reservoirs and dry, gas, and water layers.

Based on logging and testing data, a comprehensive study shows that the effective reservoir and fluid type can be effectively identified by making full use of the "excavation effect" of neutron natural gas and the difference of deep shallow bilateral resistivity (Figure 5).

(1) When the reservoir is a gas reservoir, the apparent neutron porosity is smaller than the true porosity due to the "excavation effect." However, the density data reflect the true porosity of the formation. The acoustic time difference reflects the true porosity of the formation or shows a "jump wave" phenomenon, which slightly increases. Therefore, when the neutron data overlap with the density data or the neutron data overlap with the acoustic data, there will be divergent differences. The difference between neutron porosity and acoustic porosity (density porosity) is negative, and the resistivity of both sides is "positive"

(2) When the reservoir is a water layer, the neutron has no "excavation effect," three porosity data changes are essentially the same, the interpretation results of the three porosity data are essentially the same, and the deep and shallow bilateral resistivity shows a "negative difference"

(3) When the reservoir is a dry layer or the same layer of gas and water, the neutron "excavation effect" is poor, three porosity data change is similar, interpretation results of the three porosity are essentially the same, and deep shallow bilateral resistivity is the same

Therefore, according to the characteristics of the electric logging curve of the low-resistivity gas reservoir in this area, an effective reservoir and fluid≤ identification method combining the neutron acoustic (density) discrimination method and the deep shallow dual-lateral resistivity discrimination method is established:

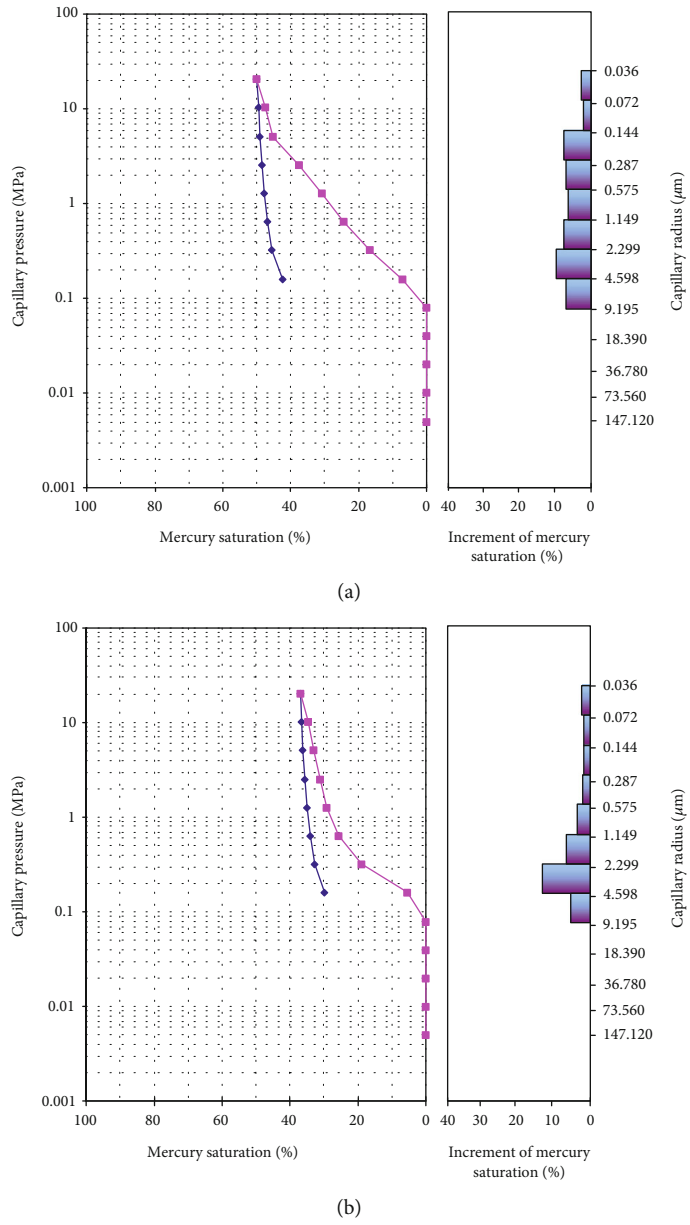

Figure 3: Capillary pressure curve and pore-throat distribution histogram of mercury deposits in the second member of the Wu 2 section in the Ke017 well area.

$$\begin{aligned}&\text{Gas layer}: \text{PORN} - \text{PORD (or PORA)}\\&\quad \le -1.4, \text{RT} - \text{RXO} \ge 1,\\&\text{Water layer}: \text{PORN} - \text{PORD(or PORA)}\\&\quad \approx 0, \text{RT} - \text{RXO} \le -2,\\&\text{Dry layer or gas-water layer}: \text{PORN} - \text{PORD(or PORA)}\\&\quad \approx 0, \text{RT} - \text{RXO} \approx 0,\end{aligned} \tag{1}$$

where PORN is the neutron porosity, PORD is the density explained porosity, PORA is the compensated acoustic wave explained porosity, RT is the formation resistivity, and RXO is the flush band resistivity.

5.1. Gas Reservoir Identification. The porosity of neutron porosity is smaller than that of the acoustic (or density) interpretation; the resistivity of the depth and shallow sides has a "positive difference" (Figure 6).

5.2. Water Level Identification. The porosity, explained by neutron porosity and sonic (or density), is large, and the resistivity of both sides has a "negative difference" (Figure 7).

5.3. Dry Layer Identification. Neutron porosity is similar to sonic (or density) interpretation porosity; the deep and shallow lateral resistivities are also similar (Figure 8).

5.4. Application Effect. According to the fluid identification method combining the neutron acoustic (density)

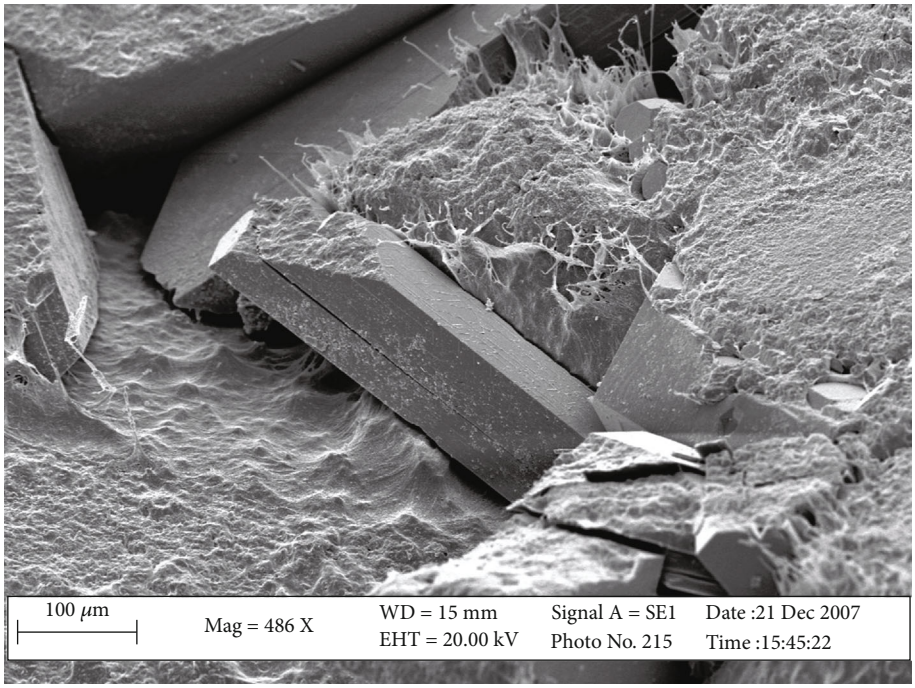

(a)

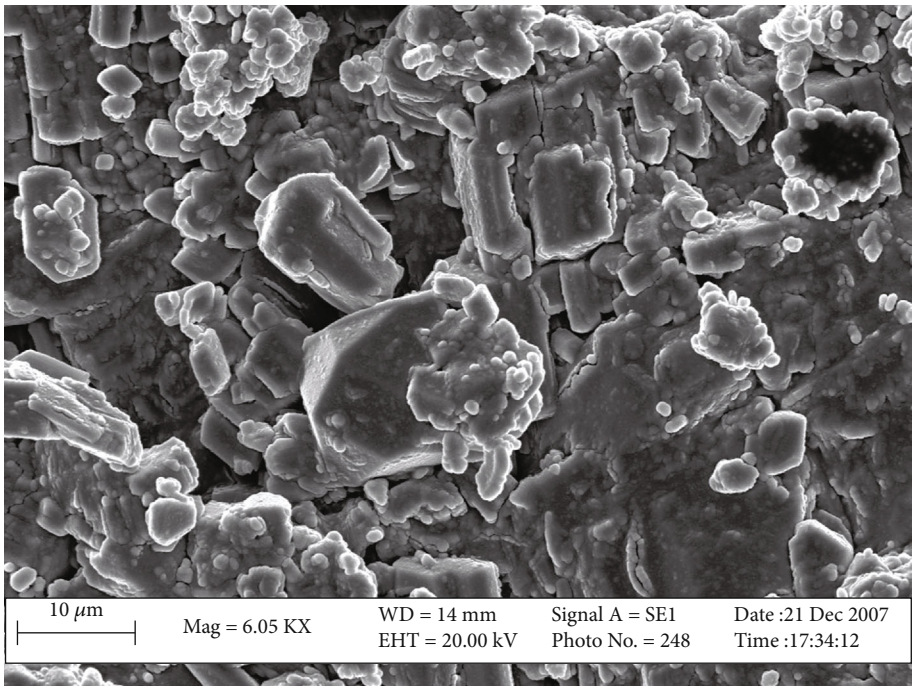

(b)

Figure 4: Continued.

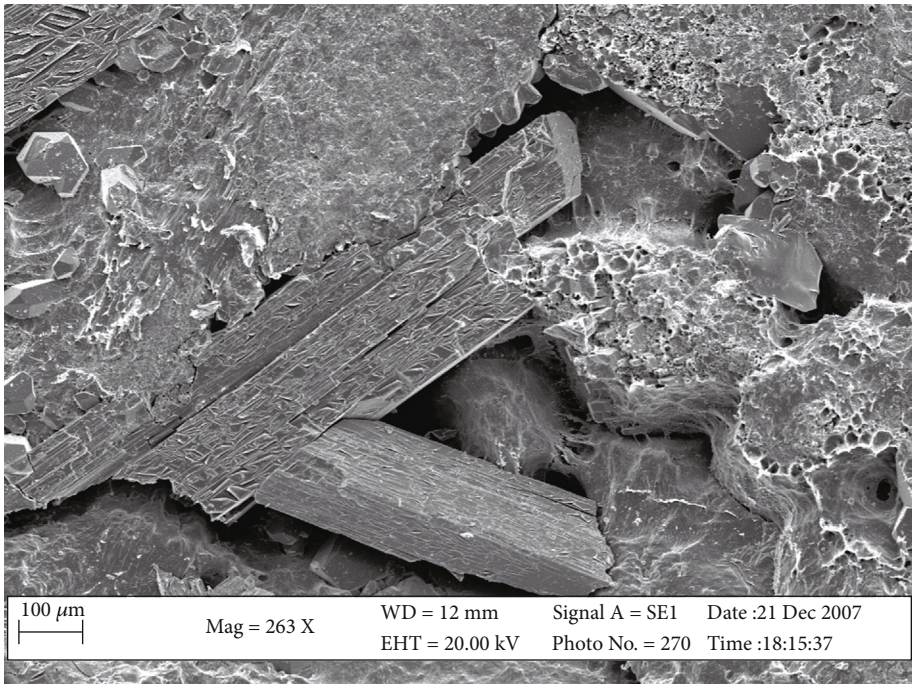

(c)

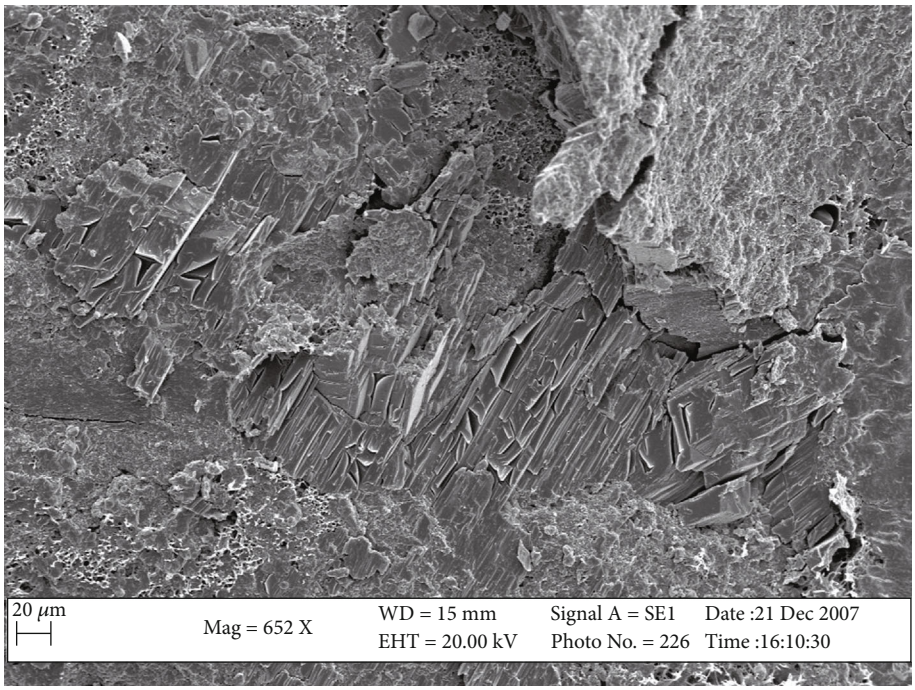

(d)

Figure 4: Scanning electron microscopy image of the Wu 2 section in the Ke017 well area. (a) Ke018, 3061.5 m, platy zeolites; (b) Ke017, 3094.33 m, equiaxed granular pyrite crystals; (c) Ke017, 3101.16 m, intergranular packing; (d) Ke018, 3064.04 m, intergranular filling.

discrimination method and deep shallow dual-lateral log resistivity discrimination method, more than 40 wells in this area and its adjacent area have been interpreted by logging. The coincidence rate of the interpretation results is as high as 90%. The application effect is significant, which effectively solves the technical problem in which the effective reservoir and fluid in this area are difficult to identify.

6. Conclusion

(1) The formation mechanism of the low-resistivity gas reservoir of the Wu 2 section in this area is due to the high content of the Iran/Mongolia mixed layer, complex pore structure, and richness in zeolite and pyrite authigenic minerals

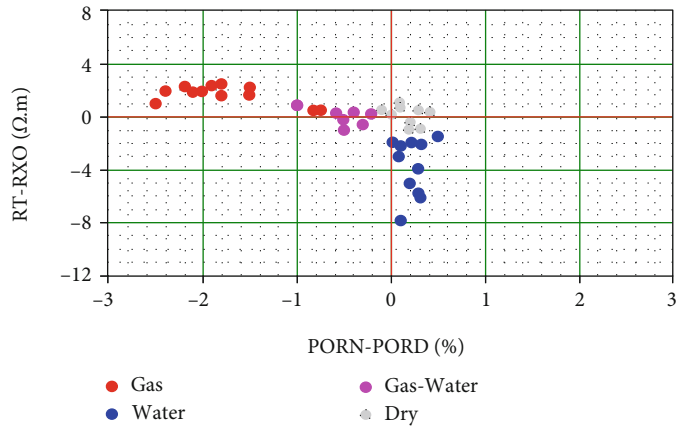

Figure 5: Intersection diagram of reservoir resistivity and difference between neutron porosity and density porosity in P_3W_2 reservoir.

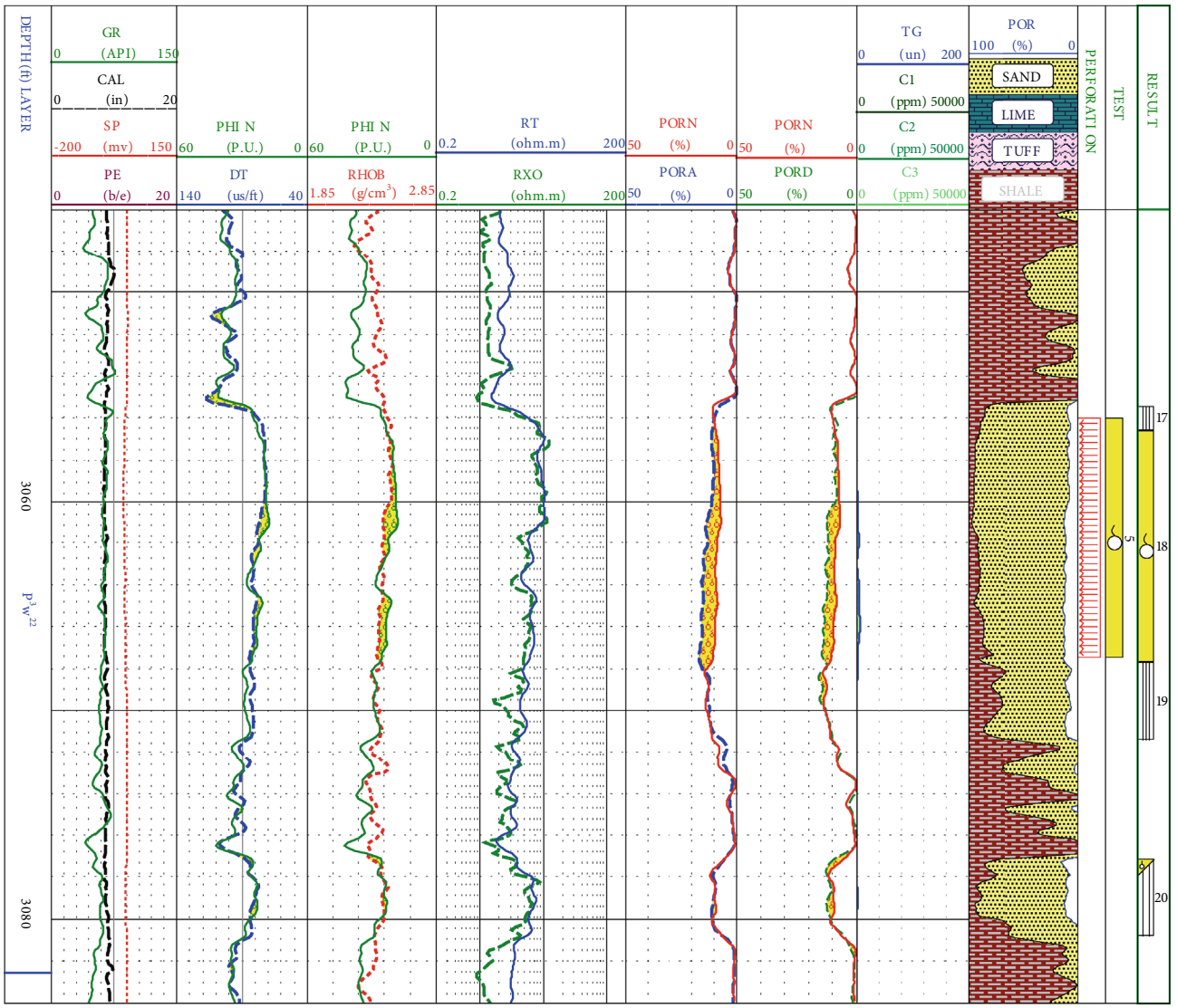

Figure 6: K58003 well logging interpretation results.

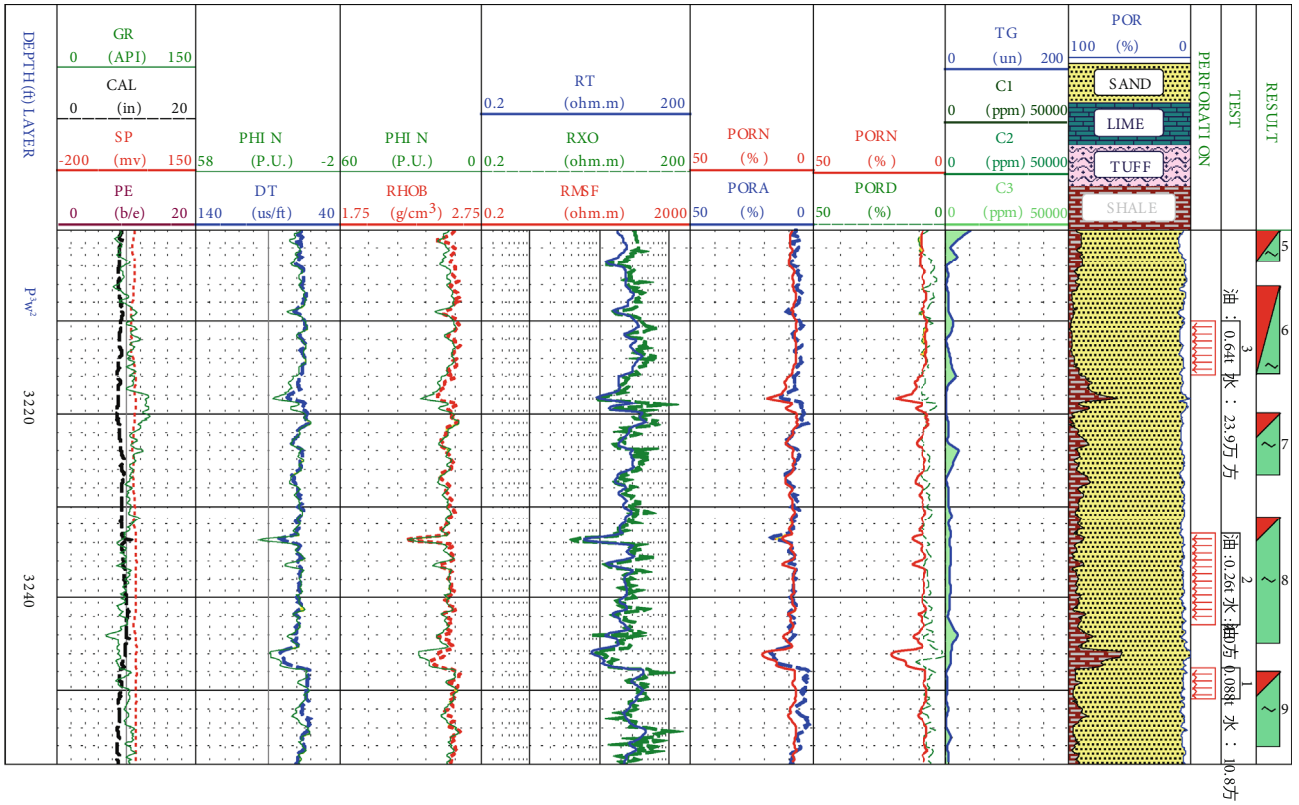

Figure 7: Log interpretation results of Ke011 well.

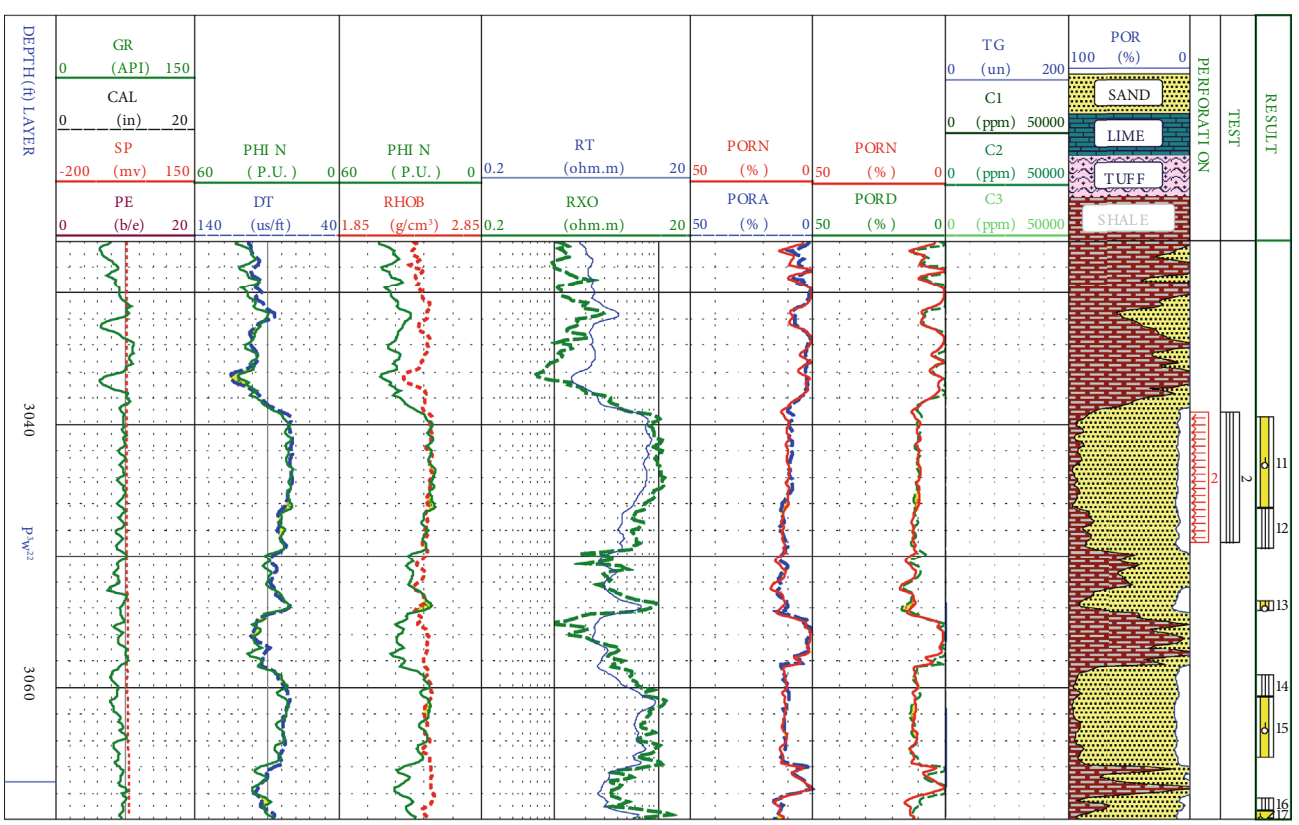

Figure 8: K58025 well logging interpretation results.

(2) The parent rock in this area is mainly volcanic clastic and the large shallow-water retrograde fan delta front sedimentary body near the source. The reservoir lithology is complex, the composition maturity and the structure maturity are low, and the original pore structure is complex. Under the complex diagenesis, the pore structure of the reservoir is more complex. The clay mineral montmorillonite transforms to the Iran/Mongolia mixed layer in large amounts and generates zeolite and pyrite authigenic minerals. Finally, a variety of genetic superimposition forms the low-resistivity gas reservoir of the Wu 2 section in this area

(3) A set of effective reservoir and fluid identification methods for low-resistivity gas reservoir is established, which combines the neutron acoustic (density) discrimination method and deep shallow dual-lateral resistivity discrimination method. It effectively solves the technical problems of logging interpretation for low-resistivity gas reservoirs in this area

Data Availability

Data will be available on request.

Conflicts of Interest

The authors declare that they have no conflicts of interest.

References

[1] China Petroleum Exploration and production Corporation, *Well logging identification method and technology of low resistivity oil & gas reservoir*, Petroleum Industry Press, Beijing, 2006.

[2] G. Yanfei, Z. Chunsheng, H. Xiaofeng, and Y. DC, "Study on formation mechanism of low resistivity gas bearing reservoir," *Lithologic Reservoirs*, vol. 23, no. 3, pp. 70–74, 2011.

[3] L. Shuiliang, X. Huiqun, L. Hong, Z. Jianghua, and Y. Huande, "Genetic mechanism and logging evaluation of low-resistivity gas reservoirs in the Tainan gas field, eastern Qaidam Basin," *Natural Gas Industry*, vol. 34, no. 7, pp. 41–45, 2014.

[4] J. Yuqiang, Z. Chun, T. Yong, G. Hongguang, X. Houwei, and J. Chunhai, "Genetic pattern of low-resistivity gas reservoirs in the Xujiahe formation, southeastern Sichuan provinces," *Oil & Gas Geology*, vol. 32, no. 1, pp. 124–132, 2011.

[5] J. Xie, X. Chai, W. Hu, Y. Jiang, and S. Yu, "Genetic mechanism of low-resistivity gas reservoirs in Sebei II gas field," *China Energy and Environmental Protection*, vol. 40, no. 2, pp. 107–112, 2018.

[6] X. G. Duan, Y. Heng, and H. H. Wang, "Genetic mechanism of upper Paleozoic low-resistivity gas reservoirs in south of Sulige gas field, Ordos Basin, China," *Journal of Chengdu University of Technology (Science & Technology Edition)*, vol. 32, no. 1, pp. 124–132, 2011.

[7] Q. X. Yu, Q. H. Lu, and Y. H. Zhu, "Characteristics and genesis of low-resistivity gas reservoir of Cretaceous-Tertiaryin southern Tianshan area," *Natural Gas Geoscience*, vol. 22, no. 1, pp. 108–114, 2011.

[8] H. Su, F. Wu, F. Meng, B. Wang, C. Yao, and Y. Xi, "Genesis of low resistivity of gas zone in Ziniquanzi formation of the southern margin of Junggar Basin," *Xinjiang Petroleum Geology*, vol. 40, no. 6, pp. 680–686, 2019.

[9] W. Jin, *Research on Gas-Water Distribution of Low Permeability Sandstone Gas Reservoir -Taking Su54 Area He8 and Shan1 Gas Reservoir as Example*, Chengdu University Technology, Chengdu, 2010.

[10] Q. Li, B. Yang, Z. Q. Yong, W. B. Fu, and X. D. Lv, "Well-logging identification of low-resistivity gas reservoirs in Hechuan area, Central Sichuan Basin," *Natural Gas Technology*, vol. 3, no. 6, pp. 44–46, 2009.

[11] X. X. Wang, F. Z. Yang, H. Z. Ma, and Y. J. Sun, "Comprehensive logging evaluation of low resistivity oil-gas reservoirs in Jabung block," *Indonesia. Natural Gas Geoscience*, vol. 20, no. 6, pp. 986–991, 2009.

[12] D. Wang, J. Qi, X. Chen, H. Tang, K. Yang, and P. Lyw, "Forming reason analysis and saturation quantitative evaluation of low- resistivity gas layer in N Gasfield of Donghai Sea," *Complex Hydrocarbon Reservoirs*, vol. 10, no. 4, pp. 7–13, 2017.

[13] L. Ma, Q. Shi, Y. Xiao, X. Wang, Z. Ji, and F. Liu, "Low-resistivity gas-bearing layer identification with DSI in Sanhu area," *Progress in Geophysics*, vol. 26, no. 2, pp. 565–571, 2011.

[14] Z. Peng, Z. Qin, H. Pan et al., "Low-resistivity gas reservoir genesis and log evaluation method in Hangjinqi area," *Natural Gas Geoscience*, vol. 27, no. 11, pp. 2054–2063, 2016.

[15] B. He, L. Ma, R. Cai, X. Hu, T. Yang, and H. Gang, "Water saturation prediction method in low resistivity tight sandstone reservoirs based on non-resistivity," *Unconventional Oil & Gas*, vol. 6, no. 6, pp. 29–40, 2019.

[16] K. Yang, L. Wang, Y. Liu, Q. Zhao, and J. Nai, "Gas-bearing properties evaluation of tight sandstone gas reservoir by array acoustic logging," *Fault-Block Oil & Gas Field*, vol. 26, no. 4, pp. 486–490, 2019.

[17] Y. Li and J. Li, "Identify low-resistivity gas reservoirs in Daniu gas field," *Natural Gas Exploration & Development*, vol. 32, no. 3, pp. 12–19, 2009.

[18] N. Luo, Y. Liu, X. He, and Y. Yang, "A method to distinguish fluid property of low-resistivity reservoir, Central Sichuan Basin," *Natural Gas Exploration & Development*, vol. 33, no. 2, pp. 26–28, 2010.

[19] L. Zhang, Y. Zhou, L. Zhao, and D. Zhang, "Finite element method using a characteristic-based split for numerical simulation of a carbonate fracture-cave reservoir," *Journal of Chemistry*, vol. 2015, Article ID 815051, 13 pages, 2015.

[20] Y. Zhao, L. Zhang, Y. Xiong, Y. Zhou, Q. Liu, and D. Chen, "Pressure response and production performance for multi-fractured horizontal wells with complex seepage mechanism in box-shaped shale gas reservoir," *Journal of Natural Gas Science and Engineering*, vol. 32, pp. 66–80, 2016.

[21] Z. Deliang, Z. Liehui, G. Jingjing, Z. Yuhui, and Z. Yulong, "Research on the production performance of multistage fractured horizontal well in shale gas reservoir," *Journal of Natural Gas Science & Engineering*, vol. 26, pp. 279–289, 2015.